Finite Element Analysis of Power Electronic Circuits Containing Nonlinear Magnetic Components

John R. Brauer
The MacNeal–Schwendler Corporation
4300 West Brown Deer Road
Milwaukee, WI 53223 USA

Abstract—**This paper presents a new finite element technique that enables nonlinear time domain analysis of power electronic circuits containing magnetic components. The new technique is first shown to compute the same voltage waveform in a nonlinear RLC circuit as previously published circuit techniques. The new technique is then demonstrated for a circuit containing an inductor with a nonlinear B–H curve, a finite conductivity, and a given geometry including air gaps.**

INTRODUCTION

Power electronic circuits often contain magnetic components operated in the nonlinear or saturated portion of their B–H curves. The magnetic components may also have significant eddy current losses. Because of the interaction between the magnetic components and the electronic components, all components must be analyzed simultaneously if the power electronic circuit designer is to predict circuit performance from schematics and drawings.

Recently, techniques have been presented that enable simulation of typical power electronic circuits containing nonlinear magnetic components [1]. Each nonlinear magnetic component is simulated using a flux linkage (λ) versus current (I) curve that is assumed known. However, such a curve is usually not known to the designer, who usually only knows the dimensions of the magnetic component and its material properties such as a B–H curve and electrical conductivity. Also, a single flux linkage curve is inadequate for the multiple windings of magnetic components such as transformers. In addition, finite conductivity of magnetic materials allows eddy current effects which are not usually included in circuit analyses [1].

This paper presents a new finite element technique that enables nonlinear time domain analysis of power electronic circuits containing magnetic components. Unlike previous finite element techniques that obtained impedances for use in circuits to obtain currents and voltages [2],[3], the finite element software discussed here enables direct coupled analysis of the magnetic component and the attached electronic circuit. After discussing the new technique, it is first applied to the nonlinear RLC circuit previously analyzed by circuit techniques [1]. Then the effects of changes in the inductor geometries and materials, including air gaps, are computed.

FINITE ELEMENT ANALYSIS INCLUDING CIRCUIT ELEMENTS

The finite element method has the capability of solving for 3D or 2D electromagnetic fields given any geometry and material properties, but it usually cannot include electric circuit components. Recently the capability of including electronic circuits in finite element analysis as "zero–dimensional (0D) finite elements" has been proposed [4]. The combined matrix equation that results from this 0D, 1D, 2D, and 3D finite element formulation is:

$$[M]\{\ddot{u}\} + [B]\{\dot{u}\} + [K]\{u\} = \{I\} \qquad (1)$$

where the matrices [M], [B], and [K] are proportional to permittivity, conductivity, and reluctivity (the reciprocal of permeability), respectively. The unknown column vector {u} is made up of magnetic vector potential $\overline{A}$ and ψ, the time integral of electric scalar potential (in volt–seconds), at nodes of finite elements. Input current excitations are contained in the right hand side {I} column vector. Equation (1) can be shown to satisfy Maxwell's equations and is solved in 3D static, frequency domain, time domain, and eigenvalue problems using the finite element program MSC/EMAS™ [5]. Finite elements available include 3D, 2D, axisymmetric, 1D (line or wire), 0D (circuit), and special open–boundary finite elements.

Zero dimensional finite elements attached to the ψ degrees of freedom of the [M], [B], and [K] matrices of (1) can represent capacitors, resistors, and inductors, respectively [4]. Each of these elements has two nodes which may be placed anywhere in space, since 0D finite elements, more commonly called circuit elements, behave the same no matter where their nodes are placed or how far apart they are.

A 0D capacitor element with capacitance C contributes to the permittance [M] matrix:

0-7803-0982-0/93 $3.00 1993 IEEE

$$[M] = C\begin{bmatrix} 1 & -1 \\ -1 & 1 \end{bmatrix} \quad (2)$$

A 0D resistor element with resistance R contributes to the conductance [B] matrix:

$$[B] = (1/R)\begin{bmatrix} 1 & -1 \\ -1 & 1 \end{bmatrix} \quad (3)$$

and a 0D inductor element with inductance L contributes to the reluctance [K] matrix:

$$[K] = (1/L)\begin{bmatrix} 1 & -1 \\ -1 & 1 \end{bmatrix} \quad (4)$$

Substituting (2), (3), and (4) into (1) gives two identical equations of the type:

$$C\frac{\partial V}{\partial t} + V/R + (1/L)\int V dt = I \quad (5)$$

where the voltage V is the difference between $\partial\psi/\partial t$ at the two nodes. Because (5) is a familiar equation of electric circuits, the zero dimensional finite element formulations have been shown to agree with electric circuit theory.

The [K] matrix of (1) can include the effects of non–linear B–H curves. The [B] matrix can include the effects of eddy currents. The [M] matrix includes the effects of displacement currents. To perform time domain analyses including nonlinear B–H effects, the Newmark Beta time–stepping technique can be used wherein nonlinear Newton–Raphson iterations are carried out at each time step or at selected time steps.

ATTACHING CIRCUITS TO MULTITURN WINDINGS IN FINITE ELEMENT ANALYSES

Finite element models can contain elements that represent each turn of wire, as has been demonstrated for one–turn primary and secondary windings on transformers attached to linear [4] and nonlinear [6] electronic circuits. In common cases of many turns on each winding, one modeling technique is to represent each individual turn with individual conducting 1D line finite elements. The 0D circuit elements may then be attached to these line finite elements. However, such a model is impractical for windings with hundreds or thousands of turns. Moreover, many hundreds or thousands of nodes would be added to the finite element models, making them inefficient to solve.

A multiturn winding technique proposed recently [7] is based upon the integral form of Faraday's Law:

$$V = -\frac{\partial}{\partial t}\int \overline{B}\cdot\overline{ds} \quad (6)$$

where the integrand is the flux linked by a coil in which the voltage V is induced. Using the definition of magnetic vector potential $\overline{A}$, we obtain:

$$V = -\frac{\partial}{\partial t}\int \nabla x\overline{A}\cdot\overline{ds} \quad (7)$$

If $\overline{A}$ is continuous, then Stokes' theorem gives:

$$V = -\frac{\partial}{\partial t}\int \overline{A}\cdot\overline{dl} \quad (8)$$

where $\overline{dl}$ is the differential vector length of the winding, which for an N turn winding is N times that of a single–turn winding.

The technique based on (8) is to model multiple turns of a winding with conducting 1D line finite elements whose nodes are constrained to the same $\overline{A}$ as the nodes of the 2D or 3D finite elements, and whose lengths are proportional to the total number of turns modeled. The 0D circuit elements are then attached directly to the elongated 1D line elements. Such techniques have recently been used for several types of transformers with attached circuits [7],[8].

NONLINEAR RLC CIRCUIT ANALYZED BY FINITE ELEMENTS FOR COMPARISON WITH OTHER WORK

Figure 1 shows an RLC circuit with a nonlinear L that has been analyzed previously by circuit techniques [1]. Figure 2 shows the applied voltage waveform [1], which is a square wave of period 50 microseconds. In this paper the circuit is analyzed by the finite element technique described above, employing 0D, 1D, and 2D finite elements in its nonlinear time–stepping solution.

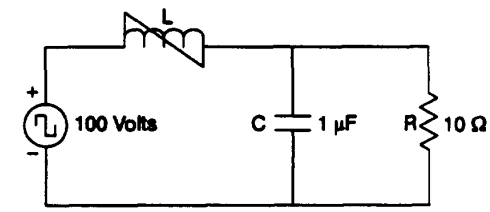

Figure 1. RLC circuit analyzed here.

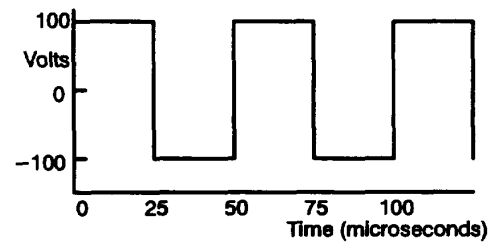

Figure 2. Input voltage waveform of Figure 1.

Figure 3 shows one example of inductor geometry that can obtain the curve of flux linkage (λ) versus current (I) curve that is given in the previous work [1]. Note that no air gaps are present in this particular design of the magnetic core. The B–H curve of the magnetic material is proportional to the previously specified piecewise linear λ–I curve [1], and is shown in Figure 4. Its conductivity is zero.

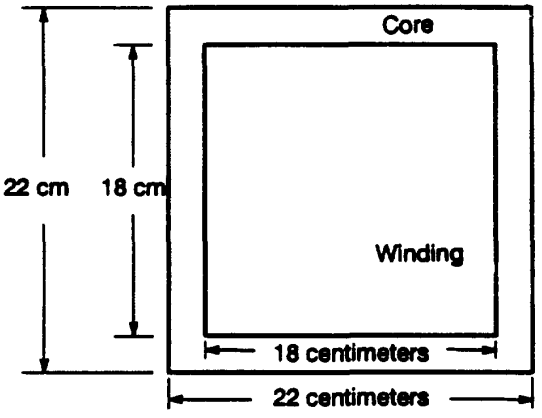

Figure 3. Geometry of inductor for Figure 1.

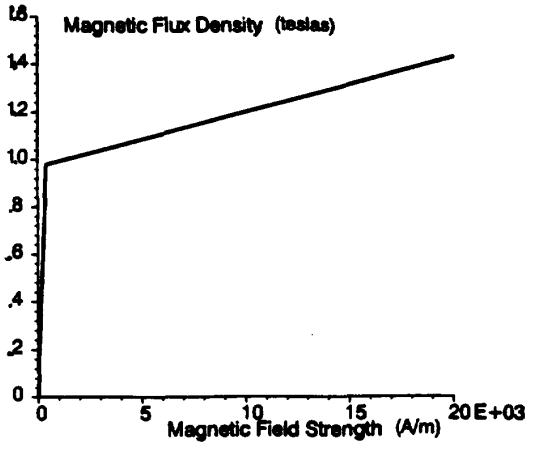

Figure 4. B–H curve assumed for core of Figure 3.

Figure 5 shows the finite element model of Figure 2. The core is modeled with 2D finite elements, to which are attached 1D wire elements to represent the multiturn winding and 0D finite elements that represent the R and C circuit elements. The square wave voltage excitation is applied via a tabular or graphical input.

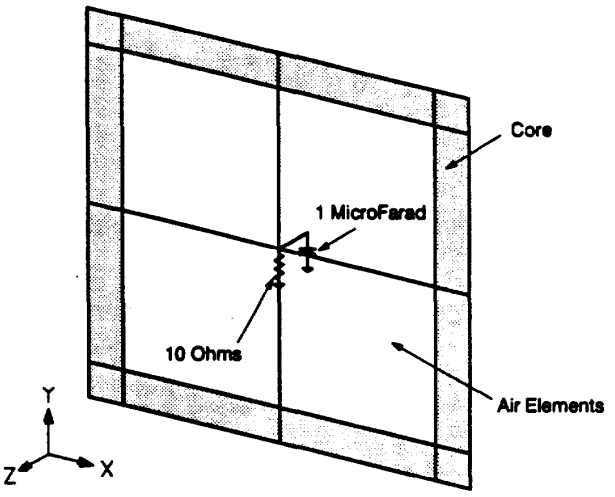

Figure 5. Finite element model of Figure 3.

Figure 6 shows the output voltage waveform (across the capacitor) computed by MSC/EMAS. The waveform appears to be identical to the waveform obtained by circuit analysis [1], thereby demonstrating the accuracy of the finite element technique.

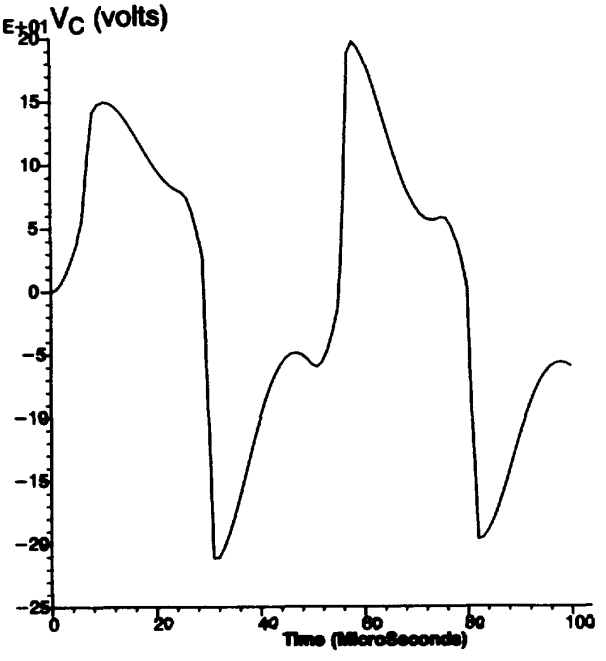

Figure 6. Output voltage waveform computed by finite element technique.

FINITE ELEMENT ANALYSIS OF CHANGES IN GEOMETRY AND MATERIALS

The advantage of the finite element method over circuit techniques is that the designer can easily investigate the effects of changes in geometry and materials. Figure 7 shows a new design of the inductor core. Note that for greater ease of assembly during manufacture, the new design has two 1 mm air gaps which enable a bobbin–wound coil to be inserted in the inductor window. To attempt to account for the greater reluctance of the added air gaps, the core now has its legs thickened to twice their thickness of Figure 3. Another change in the design is that the core material has a finite conductivity of 1 S/m, which is typical of soft ferrites. Figure 8 shows the finite element model of Figure 7.

Figure 9 shows the computed capacitor voltage waveform for the new inductor design. Note that the new waveform is considerably different from that of Figure 6. The designer may therefore want to try other geometries and materials in subsequent finite element analyses to attempt to achieve the desired waveforms of voltage and current.

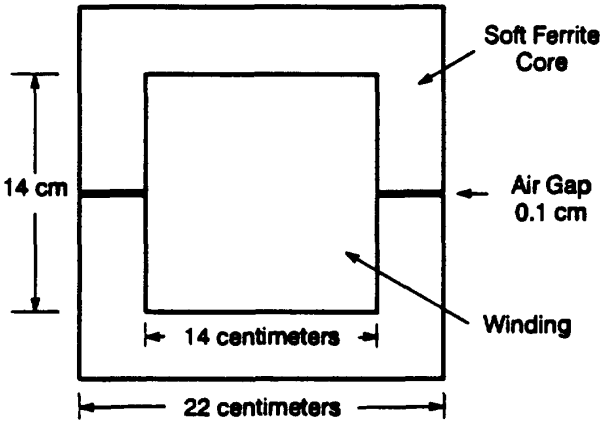

Figure 7. Geometry of new design of inductor.

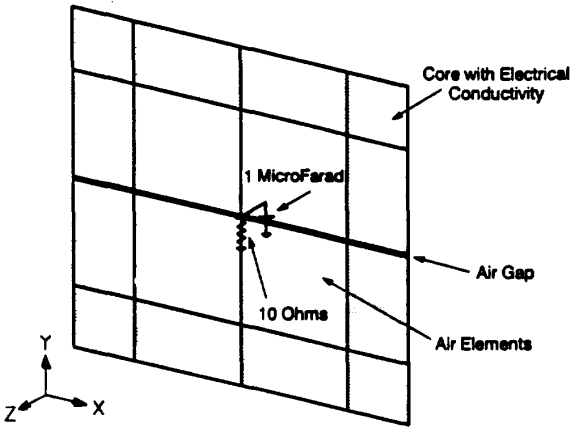

Figure 8. Finite element model of Figure 7.

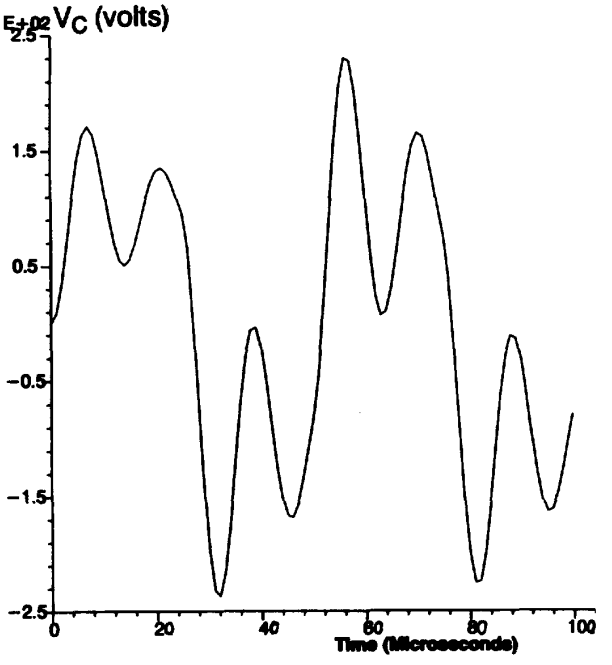

Figure 9. Output voltage waveform computed for inductor of Figure 7.

The finite element software output includes the magnetic fields and the power losses. Figure 10 shows the magnetic fluxlines in the new inductor at a typical instant. Figure 11 displays the power loss in the core versus time. A display of the locations of the power loss may also be obtained. All displays are available in color.

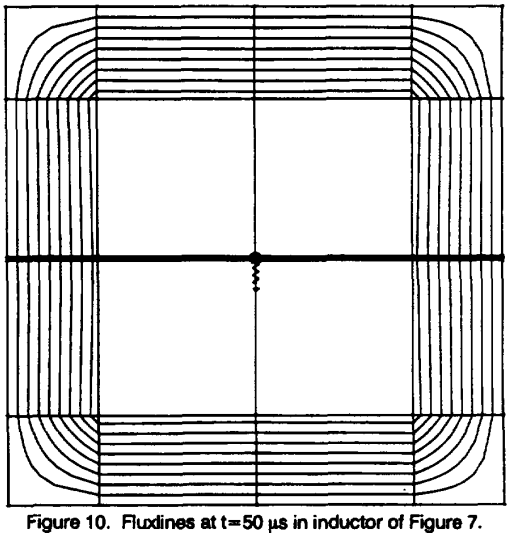

Figure 10. Fluxlines at t=50 μs in inductor of Figure 7.

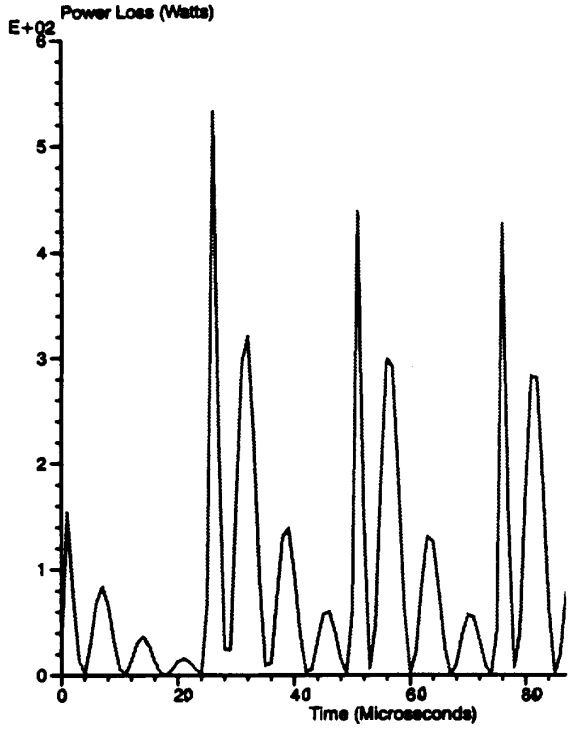

Figure 11. Core loss versus time in inductor of Figure 7.

The software also may be used for nonlinear magnetic components with multiple windings [7], such as for transformers used in power electronics. Also, 3D effects of inductors and transformers may be analyzed by using 3D finite elements. Finally, the effects of leakage flux extending to infinity may be computed by use of special finite elements that extend to infinity [9], [10].

ACKNOWLEDGMENT

The author thanks Scott E. Maurus for his valuable assistance.

CONCLUSION

A new finite element technique has been presented that directly analyzes power electronic circuits containing nonlinear magnetic components. The technique has obtained results that appear identical to those of previous circuit techniques. The new technique has also been shown able to readily compute the effects of varying geometries and material properties, which is an important advantage over circuit techniques.

REFERENCES

[1] R. M. Nelms and L. L. Grigsby, "Simulation of power electronic circuits containing nonlinear jnductances," *IEEE Trans. Aerospace & Electronic Systems*, Nov. 1991, pp. 924–931 ("based on a paper presented at the 1990 Applied Power Electronics Conference").

[2] John R. Brauer (ed.), *What Every Engineer Should Know About Finite Element Analysis*, Marcel Dekker, Inc., New York, 1988, p. 121.

[3] Rudy Severns, "Additional losses in high frequency magnetics due to non ideal field distributions," *APEC Conference Proceedings*, 1992, pp. 333–338.

[4] J. R. Brauer, B. E. MacNeal, L. A. Larkin and V. D. Overbye, "New method of modeling electronic circuits coupled with 3D electromagnetic finite element models," *IEEE Trans. on Magnetics*, v. 27, September 1991, pp. 4085–4088.

[5] B. E. MacNeal, J. R. Brauer, and R. N. Coppolino, "A general finite element vector potential formulation of electromagnetics using a time–integrated electric scalar potential," *IEEE Trans. on Magnetics*, v. 26, September 1990, pp. 1768–1770.

[6] R. H. Vander Heiden, A. A. Arkadan, J. R. Brauer, and G. T. Hummert, "Finite element modeling of a transformer feeding a rectified load: the coupled power electronics and magnetic field problem," *IEEE Trans. on Magnetics*, v. 27, Nov. 1991, pp. 5217–5219.

[7] John R. Brauer and Bruce E. MacNeal, "Finite element modeling of multiturn windings with attached electric circuits," *IEEE Trans. on Magnetics*, v. 29, March 1993, in press.

[8] S. Ratnajeevan H. Hoole (ed.), *Finite Elements, Electromagnetics, and Design*, chapter by B. E. MacNeal and J. R. Brauer, PIER book series, Elsevier Science Publishers, Amsterdam, in press.

[9] J. R. Brauer, S. M. Schaefer, J. F. Lee, and R. Mittra, "Asymptotic boundary condition for three dimensional magnetostatic finite elements," *IEEE Trans. on Magnetics*, v. 27, November 1991, pp. 5013–5015.

[10] John R. Brauer and Franz Hirtenfelder, "Surface integrals on 3D and 2D finite element models for skin effect excitations and open boundaries," *IEEE Trans. on Magnetics*, v. 28, March 1992, pp. 1659–1662.